USE OF GEOSTATISTICS TO INTEGRATE INTERFEROMETRIC SAR DATA WITH LEVELING MEASUREMENTS OF LAND SUBSIDENCE

Alfred Stein[a,*]*and Yueqin Zhou[a]
[a] ITC, International Institute for Geo-Information Science and Earth Observation
PO Box 6, 7500 AA Enschede
The Netherlands

PS ICWG II/IV Automated Geo-spatial Data Production and Updating

Abstract D-InSAR data of ground surface deformation have uncertainty caused by several sources associated with image acquisitions and data processing. In this study, these data are modeled as the sum of a trend, a zero-mean stochastic process and white noise. The aim is to improve their accuracy by correcting the errors using measurements as the ground truth. A geostatistical approach integrates D-InSAR subsidence data with *in situ* leveling measurements. Discrepancies between the true subsidence values and original D-InSAR measurements are analyzed at leveling points using variograms and predicted at unvisited points using kriging. The proposed method is applied to the data collected in the where land subsidence occurs due to groundwater extraction in the Tianjin area in China. Results demonstrate the capability of D-InSAR to detect subsidence at the cm-level, and of using a limited number of leveling points to improve the accuracy of D-InSAR deformation measurements provided the coherence of images used is high enough. In addition, localization of leveling points is optimized.

*Corresponding author

1 Introduction

Synthetic Aperture Radar (SAR) is an active remote sensing system, operating in the microwave region of the electromagnetic spectrum. It emits a series of coherent, pulsed electromagnetic waves from an antenna mounted on an airborne or spaceborne vehicle, and records amplitude and phase of backscattered signals from objects on the ground (Hanssen 2001; Zhou et al., 2003). In this sense, SAR systems acquire complex images. The deformation of the ground surface, such as earthquake displacements, land subsidence caused by groundwater, natural gas, or oil extraction, can be quantified by comparing the phase information of two complex SAR images of which the first is recorded before deformation, and the second thereafter. This is done using differential SAR interferometry (D-InSAR). D-InSAR provides a deformation image on a pixel-by-pixel basis over an area of thousands of square kilometers.

Traditionally, leveling is used for measuring vertical deformation, i.e. subsidence and uplift, at a spatially discrete set of locations along trajectories. It is followed by interpolation to get a continuous two-dimensional coverage. The accuracy is high at measurement points, but may be low at non-measured points. Besides, for a non-homogeneous deformation pattern, point-wise leveling measurements may not always be effective to represent deformation, unless points are measured at a very high density.

So far, D-InSAR has not been as widely used as leveling. The main reason is that it produces noise and causes artifacts during data acquisition and processing. Noise is created by decorrelation between two or more images acquired at different times, whereas spatial and temporal variation in the atmosphere creates artifacts that are difficult to distinguish from ground deformation. For these reasons, D-InSAR accuracy may be too low to detect small deformations. Although error sources are inevitable in differential SAR interferometry, their effects can be reduced.

Several studies show an agreement between DInSAR measurements and leveling results in detecting land subsidence (e.g., Carnec and Fabriol 1999), but both can be ineffective if used alone. If only vertical deformation occurs, a solution is to combine D-InSAR with leveling as recommended by Van der Kooij (1995) and Van Bree et al. (1999). As an alternative, Zhou et al. (2000) use a set of sparsely distributed leveling measurements as the ground truth, and fit a polynomial model to the differences between the two kinds of measurements at test points

In this study we further integrate data obtained with InSAR and those obtained with leveling. The objective is to correct the errors contained in D-InSAR measurements by using measurements as the ground truth to improve their accuracy. We propose the use of geostatistics to integrate leveling with D-InSAR. Geostatistics is well suited to deal with data that are neither deterministic nor purely random, and show spatial correlation. The spatial correlation is estimated by variograms, which in turn are used to estimate deformation at non-measured locations (Chils and Delfiner 1999). The proposed method is applied to data collected in Tianjin Municipality, China, where land subsidence occurs due to groundwater extraction.

2 Materials and Methods

2.1 Height change measurements by differential SAR interferometry

Differential SAR interferometry creates two interferograms (phase differences) from single look complex (SLC) SAR images. The first interferogram results from two images spanning a relatively long time interval. If the interferogram is used to detect land subsidence between two image acquisitions, it contains fringes due to both topographic effects and height changes. The second interferogram comes from two SAR images spanning a relatively short time interval, say, one day, or is calculated from an external Digital Elevation Model (DEM), and contains topographic fringes only. By differencing the two interferograms, topographic effects are removed, and only height change effects remain.

2.2 Integration of leveling and D-InSAR measurements using geostatistics

Let $Dh_s(x)$ be a height change measurement obtained with D-InSAR at a two-dimensional coordinate vector x (the center of a pixel). Taking the different types of errors in the measurement into account, we model $Dh_s(x)$ by the expression

$$Dh_s(x) = Dh(x) + m_s(x) + \epsilon_s(x) + e_s(x) \qquad (1)$$

where $Dh(x)$ denotes the true height change at x, and $m_s(x)$ and $\epsilon(x)$ constitute the systematic distortion. The term $m_s(x)$ models the bias mainly due to mean atmospheric effects and possible indetermination of the orbital parameters, $\epsilon(x)$ is the spatially correlated error caused by local atmospheric effects and uncertainty in topographic correction. We assume that $Cov(\epsilon(x), \epsilon(x+h) = C_\epsilon(h)$, $C_\epsilon(h)$ being a covariance function, depending only on distance h. Systematic distortion is estimated during post-processing, yielding an estimate for the true height change and additive white noise after subtraction. A calibrated raster height change map is generated on the basis of height change measurements corrected for systematic distortion.

In situ leveling height change measurements at a set of points from the same area can be used for calibration. Let $Dh_L(x)$ be the leveling height change at location x, then

$$Dh_L(x) = Dh(x) + e_L(x) \quad (2)$$

where $e_L(x)$ is the error term modeling errors from leveling surveying. We apply a somewhat simpler model for these data as the bias is negligible and errors are mainly non-spatial in nature. If leveling and D-InSAR height change measurements are available at the same location, then from equations 1 and 2 we obtain:

$$\Delta = Dh_S(x) - Dh_(x) = m_s(x) + \epsilon_s(x) + e(x) \quad (3)$$

where $e(x) = e_S(x) - e_L(x)$ is the independent error part. In terms of geostatistics, the term $m_S(x)$ in equation 3 is the trend (or drift) that can be modeled by a kth-order polynomial, $\epsilon(x)$ is a zero-mean stationary process, and $e(x)$ is the error related to measurement errors in data collection and/or micro variations.

If sufficient number of well distributed leveling points are available, $m_S(x)$ and $\epsilon_S(x)$ can be modeled based on their leveling and D-InSAR measurements using a geostatistical approach. This is then followed by a geostatistical interpolation to create a map.

3 Applications and results

3.1 Data

The proposed method is applied to data collected in Tianjin Municipality, China. The city is located at the coast of Bohai Gulf, and has experienced the most serious subsidence in China since 1959 due to groundwater extraction. The total subsidence area is approximately equal to 13,000 km^2 and consists of five subsidence centers. In the urban area, the maximum accumulative subsidence between 1959 and 1986 exceeds 2.5m, whereas the average rate of subsidence between 1980 and 1986 equals 13.5 $cmyr^{-1}$. By adopting water conservation measures, including closing some wells and refilling water into underground layers, the rate of subsidence reduced to 2 $cmyr^{-1}$. Further industrial development, however, has stimulated groundwater extraction in the suburban area, leading in those areas to a subsidence rate of 5-8 $cmyr^{-1}$. To monitor subsidence, an elaborate network of monitoring sites was established in 1986 (figure 1). Since then, a leveling campaign has been carried out once every year mostly in the month of October. In total, six phases of leveling measurements (1992 - 1997) of the network have been collected. They indicate a set of points with planar coordinates in an arbitrary coordinate system and a series of height values measured at different times. Two tandem pairs of ERS-1/2 SLC SAR images covering the urban area of the city, acquired in 1996 and 1997, respectively, have been collected as well. The spatial baselines as well as time differences of the images are listed in table 1.

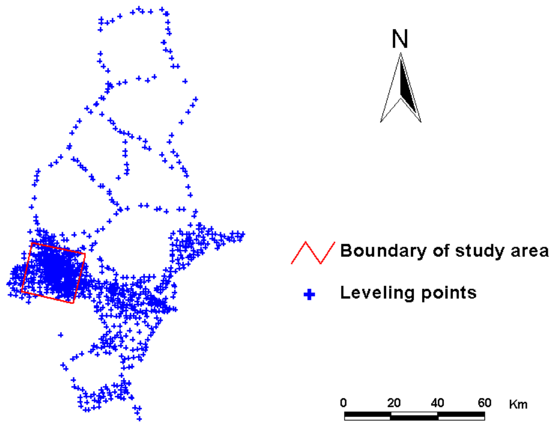

Figure 1: The leveling network established in Tianjin to monitor land subsidence. The total length of the leveling routes equals 3,000 km. The study area is indicated by a rectangular boundary.

I_1	I_2	I_3	I_4
97/10/02	97/10/03	96/01/11	96/01/12
ERS-1	ERS-2	ERS-1	ERS-2
32499	12826	23481	03808
0	-228/-329	-190/-252	-148/-150

Table 1: Differential SAR interferometric images $I_1 \ldots i_4$ collected at several dates (first row), by two satellites (second line), at different orbits (third line) and different baselines ($B_\perp/B_\parallel$) (fourth line).

3.2 Integration

Among the 399 leveling points, 173 points selected at random are used as test points, and 226 others are used as control using cross-validation. At all leveling locations the discrepancies between D-InSAR and leveling measurements are calculated using equation 3. Systematic distortion is predicted for each extracted coherent pixel, and subtracted from the original D-InSAR measurements. The contour map based on the calibrated D-InSAR measurements is shown in figure 2. A comparison using boxplots and residual variograms is made with (a) original D-InSAR measurements and (b) error-detrended measurements. Box plots of discrepancies at 226 control points

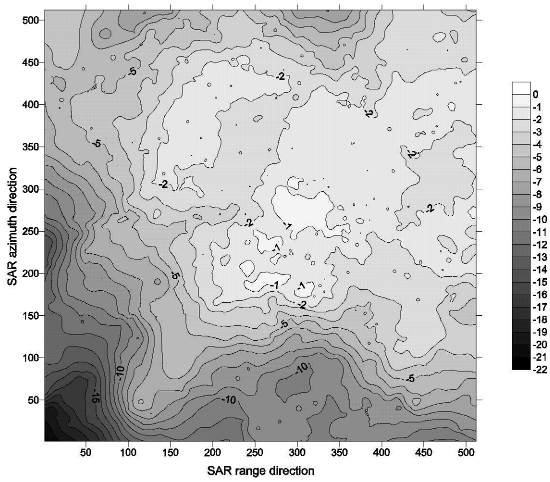

Figure 2: Contour map generated from the calibrated D-InSAR height change measurements (cm). Coordinates are expressed in pixels with a size of 40 by 40 m.

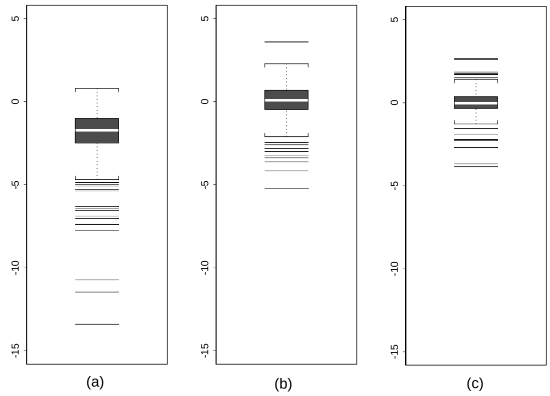

Figure 3: Box plots of the discrepancies of leveling measurements with (a) original D-InSAR measurements, (b) error-detrended measurements, and (c) integrated measurements.

are given in figures 3(a – c). These show that the number of outside values of errors decreases following calibration, whereas symmetry increases. Directional variograms of the discrepancies (figures 4(a–c)) show a trend contained in the discrepancies of the original D-InSAR measurements since the variograms are unbounded, particularly in the SAR range direction (azimuth=90). This trend is not present in the other two approaches. For the original data, the mean error equals 2.1, which reduces for the detrended and the integrated results to 0.0. Meanwhile, the root mean square error (RMSE) is equal to 2.8 for the original data, 1.1 for the detrended measurements and 0.8 for the integrated results. Notice that these values are not directly comparable, as the data are of a different type. Data detrending removes the trend part of the systematic distortions and decreases the RMSE value, but the spatially correlated errors still remain. The correlation length is approximately 180 pixels (7 km). By removing the spatially correlated errors predicted using kriging, both the RMSE and the correlation length decrease.

4 Conclusion

This paper describes a geostatistical approach of combining D-InSAR with in situ leveling measurements. This approach allows a reduction of the RMSE provided that high enough coherence of the associated images is ensured and a number of in situ leveling measurements are available. It also allows a considerable reduction of the amount of leveling benchmarks particularly in a large area.

References

Carnec, C AND Fabriol, F. 1999. Monitoring and modeling land subsidence at the Cerro Prieto geothermal field, Baja California, using SAR interferometry. Geophys. Letters., 26, 9, 1211-1214.

Chilès, J. P., and Delfiner, P., 1999, Geostatistics: modeling spatial uncertainty (New York: Willy & Sons).

Hanssen, R.F. 2001 Radar interferometry: data interpretation and error analysis. Kluwer, Dordrecht.

Van der Kooij, M. W. A., Van Halsema, D., Groenewoud, W., Mets, G. J., Overgaauw, B., and Visser, P. N. A. M., 1995, SAR land subsidence monitoring. NRSP-2 95-13, Dutch Remote Sensing Board (Delft: BCRS).

Van Bree, R. J. P., Gens, R., Groot, J. S., Van Halsema, D., Hanssen, R. F., Van Den Hout, P., Klees, R., De Min, E. J., Schrama, E. J. O., and Usai, S., 1999, Deformation measurements with SAR. USP-2 9-16, Dutch Remote Sensing Board (Delft: BCRS).

Zhou, Y., Molenaar, M., and Li, D., 2000, Integrated use of interferometric SAR data and leveling measurements for monitoring land subsidence, ISPRS 2000 congress: geoinformation for all, 16-23 July 2000, Amsterdam. (Lemmer: GITC), pp. 9–16.

Zhou, Y., A. Stein and M. Molenaar. 2003. Integrating interferometric SAR data with levelling measurements of land subsidence using geostatistics. International Journal of Remote sensing 24, 3547 – 3564

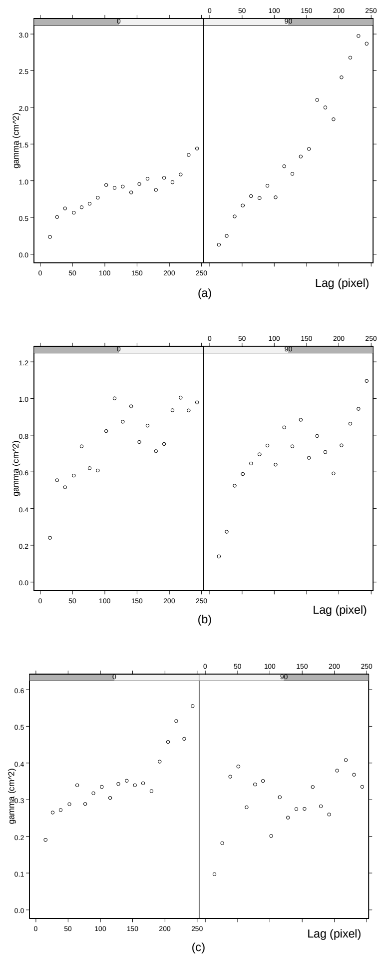

Figure 4: Directional variograms of the discrepancies of leveling measurements with (a) original D-InSAR measurements, (b) error-detrended measurements, and (c) integrated measurements.